Magazine of Concrete Research
Volume 69 Issue 5

Shear friction strength of monolithic concrete interfaces
Kwon, Yang, Hwang and Ashour

Magazine of Concrete Research, 2017, **69**(5), 230–244
http://dx.doi.org/10.1680/jmacr.16.00190
Paper 1600190
Received 24/08/2016; revised 28/08/2016; accepted 22/09/2016
Published online ahead of print 01/11/2016
Keywords: joints/shear/structural design

ice Institution of Civil Engineers
publishing

Shear friction strength of monolithic concrete interfaces

Seung-Jun Kwon
Department of Civil & Environmental Engineering, Hannam University, Daejeon, South Korea

Keun-Hyeok Yang
Department of Plant Architectural Engineering, Kyonggi University, Suwon, South Korea (corresponding author: yangkh@kgu.ac.kr)

Yong-Ha Hwang
Department of Architectural Engineering, Kyonggi University, Suwon, South Korea

Ashraf F. Ashour
School of Engineering, University of Bradford, Bradford, UK

This paper presents an integrated model for the shear friction strength of monolithic concrete interfaces derived from the upper-bound theorem of concrete plasticity. The model accounts for the effects of applied axial stresses and transverse reinforcement on the shear friction action at interfacial shear cracks. Simple equations are also developed to generalise the effectiveness factor for compression, the ratio of effective tensile to compressive strengths and the angle of concrete friction. The reliability of the proposed model is verified through comparisons with previous empirical equations and 103 push-off test specimens compiled from different sources in the literature. The previous equations considerably underestimate the concrete shear transfer capacity and the underestimation is notable for interfaces subjected to additional axial stresses. The proposed model provides superior accuracy in predicting the shear friction strength, resulting in a mean between experimental and predicted friction strengths of 0·97 and low scatter. Moreover, the proposed model shows consistent trends with the test results in evaluating the effects of various parameters on the shear friction strength.

Notation

A_c	section area of shear failure plane
A_{vf}	area of transverse reinforcement across shear failure plane
c_0	reference aggregate size (= 25 mm)
d_a	maximum size of aggregate
f'_c	concrete compressive strength
f^*_c	effective compressive strength of concrete
f_{co}	reference concrete compressive strength (= 10 MPa)
f_t	concrete tensile strength
f^*_t	effective tensile strength of concrete
f_y	yield strength of transverse reinforcement
N_x	axial load normally applied to the shear plane of concrete interface
V_n	shear force in shear plane of concrete interface
W_E	external work done by applied load
W_I	internal energy dissipated along failure plane
X_{ic}	horizontal coordinate of instantaneous centre
α	angle between relative displacement at the chord midpoint and failure plane
α_f	angle between transverse reinforcement and shear plane
γ	ratio of test results and predictions
γ_m	mean of γ values
γ_s	standard deviation of γ values
γ_v	coefficient of variation of γ values
δ	relative displacement
ε_u	ultimate strain of concrete in compression
ε_{tu}	ultimate strain of concrete in tension
θ_s	angle of transverse reinforcement relative to the failure plane
λ	modification factor for lightweight concrete
μ	coefficient of friction
ν_c	effectiveness factor for concrete compressive strength
ν_t	effectiveness factor for concrete tensile strength
ρ_c	unit weight of concrete
ρ_o	reference unit weight of concrete (= 2300 kg/m^3)
ρ_{vf}	transverse reinforcement ratio
σ_x	axial stress normally applied to the shear plane
τ_n	shear friction strength in shear plane
ϕ	friction angle of concrete
ω	relative rotational displacement of rigid block I to rigid block II about IC
ω_v	transverse reinforcement index

Introduction

The load transfer at shear interfaces occurring in connections between columns and corbels, between squat shear walls and columns, of dapped end beams and shear keys is governed by the shear friction action (ACI-ASCE Committee 426, 1973). The shear friction strength of concrete depends on the roughness and aggregate interlock at shear cracks developed along the interface and the magnitude of axial stresses applied to the interface. The provisions set out by the American Association of State Highway and Transportation Officials (Aashto)

(Aashto, 2012) and other shear friction models (Haskett *et al.*, 2010; Mattock, 2001; Walraven *et al.*, 1987) indicate that the shear transfer capacity of concrete is governed by the frictional resistance including aggregate interlock and the cohesion of cementitious materials along shear cracks. Hence, the shear friction capacity of lightweight concrete (LWC) is commonly lower than that of normal-weight concrete (NWC) having the same compressive strength (Sagaseta and Vollum, 2011; Yang *et al.*, 2012). The shear transfer capacity of reinforcing bars crossing the interfaces is also influenced by the frictional resistance of concrete, because tensile stresses in the reinforcement depend on the relative slip along the interface (Ali and White, 1999). This means that the rupture of aggregate particles owing to crack propagation results in a reduction of the coefficient of friction of concrete and tensile stresses generated in the transverse reinforcement. Overall, the shear friction resistance at interfacial cracks needs to be determined considering the variations in the coefficient of friction of concrete according to the unit weight and compressive strength of concrete. However, the mechanical diversity of the shear friction of different concrete types is undervalued in most previous models (Loov and Patnaik, 1994; Mattock, 2001; Shaikh, 1978; Walraven *et al.*, 1987) because they were empirically formulated using limited test data with a narrow range of unit weight or compressive strength of concrete.

A few researchers have developed numerical techniques to evaluate the shear friction capacity of concrete using the upper-bound theorem of plasticity theory (Nielsen and Hoang, 2011; Yang *et al.*, 2012). The shear friction action of different concrete types at interfacial shear cracks can be successfully explained using concrete plasticity. Yang *et al.* (2012) demonstrated that the friction angle and cohesion of concrete can be formulated as a function of the ratio of effective tensile and compressive strengths of concrete, assuming that concrete can be modelled as a rigid perfectly plastic material obeying modified Coulomb failure criteria. Thus, the main objectives of the present study were as follows.

(*a*) To extend the approach developed by Yang *et al.* (2012) to account for the effects of applied axial stresses and transverse reinforcement on the shear friction action at interfacial shear cracks.
(*b*) To produce a comprehensive database of shear friction strength of concrete measured from testing of push-off specimens of different concrete types.
(*c*) To evaluate the reliability of the empirical equations of code provisions (Aashto, 2012; ACI, 2014) and previous researchers (Loov and Patnaik, 1994; Mattock, 2001; Shaikh, 1978; Walraven *et al.*, 1987) against the comprehensive database collected.
(*d*) To study the effect of different parameters on the shear friction strength of concrete using the Aashto equation and the proposed mechanism model and the test results extracted from the collected database.

Mechanism analysis

Failure mechanism

Experimental investigations (Ahmed and Ansell, 2010; Hofbeck *et al.*, 1969; Mattock and Hawkins, 1972; Yang *et al.*, 2012) have shown that a monolithic concrete interface under direct shear and axial loads usually separates into two rigid blocks at failure, as shown in Figure 1. The failure zone between the concrete blocks can be generally idealised as a hyperbolic yield line, as proved by Ashour and Morley (1994). One rigid block has two translational and rotational displacement components relative to the other rigid block. Thus, one rigid block can be assumed to be rotating about an instantaneous centre (IC). For the idealised failure mechanism, the interfacial shear plane at failure can be regarded as a plane strain problem, as lateral (out of plane) strains are prevented under the same condition of the failure section (Nielsen and Hoang, 2011; Yang *et al.*, 2012).

Upper-bound solution

The upper-bound analysis uses the energy principle to calculate the shear friction strength for the kinematically admissible failure mechanism explained above. The external work (W_E) done by the applied shear (V_n) and axial loads (N_x) is

$$1. \quad W_E = V_n \omega X_{ic} - N_x \omega X_{ic} \tan \alpha$$

where ω is the relative rotational displacement of rigid block I to rigid block II about the IC, X_{ic} is the horizontal coordinate of the IC and α is the angle between the relative displacement (δ) at the midpoint of the hyperbolic yield line chord and the failure plane chord. The sign of the external work done by N_x becomes negative as N_x has an opposite direction to the propagation of the relative displacement. For a plane strain problem, the internal energy (W_I) dissipated in concrete and transverse reinforcement along the failure surface is estimated from the

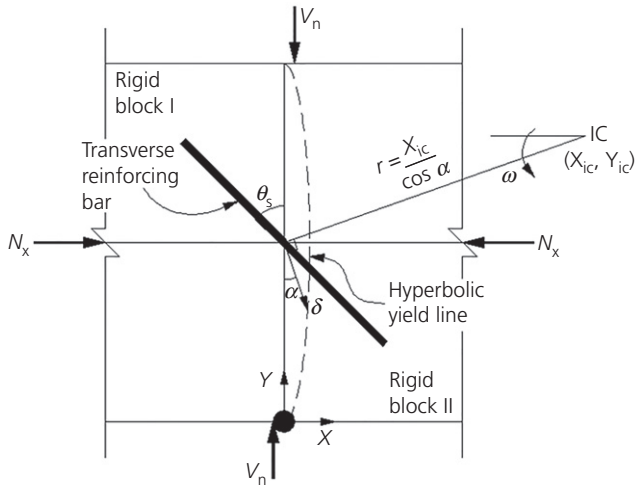

Figure 1. Idealised failure mechanism of a monolithic concrete interface

following general formula (Yang *et al.*, 2012)

$$W_I = \frac{1}{2} f_c^* \delta (l - m \sin\alpha) A_c + A_{vf} f_y \delta \cos(\theta_s - \alpha) \quad (2)$$

in which

$$l = 1 - 2\frac{f_t^*}{f_c^*}\frac{\sin\phi}{1-\sin\phi}$$

$$m = 1 - 2\frac{f_t^*}{f_c^*}\frac{1}{1-\sin\phi}$$

$f_c^* (= v_c f_c')$ and $f_t^* (= v_t f_t)$ are respectively the effective compressive and tensile strengths of concrete, v_c and v_t are respectively the effectiveness factors for concrete in compression and tension, f_c' and f_t are respectively the compressive and tensile strengths of concrete, A_c is the area of failure plane, A_{vf} and f_y are respectively the area and yield strength of the transverse reinforcement at the failure plane, θ_s is the angle of transverse reinforcement relative to the failure plane and ϕ is the friction angle of concrete. The relative displacement can be also written as $\omega(X_{ic}/\cos\alpha)$. Applying the energy conservation principle, the shear friction strength (τ_n) of monolithic concrete interfaces can be arranged in the following form

$$\tau_n = \frac{V_n}{A_c} = \frac{1}{2} f_c^* \frac{1}{\cos\alpha}(l - m\sin\alpha) + \rho_{vf} f_y \frac{[\cos(\theta_s - \alpha)]}{\cos\alpha} + \sigma_x \tan\alpha \quad (3)$$

where ρ_{vf} is the transverse reinforcement ratio and σ_x is the additional axial stress normally applied to the interfaces. In accordance with the upper-bound theorem, the collapse load can be determined by considering the differential equation, $\partial\tau_n/\partial\alpha = 0$, which gives

$$\alpha = \sin^{-1}\left[\frac{1}{l}\left(m - \frac{2(\rho_{vf} f_y \sin\theta_s + \sigma_x)}{f_c^*}\right)\right] \quad (4)$$

Effectiveness factor for compression and effective strength ratio

To transform concrete with quasi-brittleness into an equivalent rigid perfectly plastic material obeying modified Coulomb failure criteria, effectiveness factors are introduced and calculated by equating the area of the rigid perfectly plastic stress–strain curve to that of the actual stress–strain curve of concrete. Hence, the values of v_c and v_t can be determined using (Exner, 1979)

$$v_c = \frac{f_c^*}{f_c'} = \int_0^1 \left(\frac{\sigma_c}{f_c'}\right) d\left(\frac{\varepsilon_c}{\varepsilon_u}\right) \quad (5)$$

$$v_t = \frac{f_t^*}{f_t} = \int_0^1 \left(\frac{\sigma_t}{f_t}\right) d\left(\frac{\varepsilon_t}{\varepsilon_{tu}}\right) \quad (6)$$

where σ_c is the compressive stress corresponding to compressive strain ε_c, ε_u is the ultimate compressive strain, σ_t is the tensile stress corresponding to tensile strain ε_t and ε_{tu} is the ultimate tensile strain.

Yang *et al.* (2012) determined the effectiveness factors based on modified versions of the compressive stress–strain relationship generalised by Thorenfeldt *et al.* (1987) and the tensile stress–strain relationship derived by Hordijk (1991). In this study, the model proposed by Yang *et al.* (2014) was used for the compressive stress–strain relationship to cover the extensive range of unit weight (ρ_c = 1400–4000 kg/m^3) and compressive strength (f_c' = 10–100 MPa) of concrete. The fundamental procedures to solve Equations 5 and 6 are specifically explained in the previous study (Yang *et al.*, 2012).

The effectiveness factor of concrete in compression (v_c) is significantly affected by the compressive strength and unit weight of concrete, yet independent of the maximum aggregate size (Yang *et al.*, 2012). For concrete with f_c' = 20–100 MPa and ρ_c = 1400–4000 kg/m^3, Equation 5, using the compressive stress–strain relationship proposed by Yang *et al.* (2014), was used and then non-linear multiple regression (NLMR) analysis was carried out in order to propose a simple equation for v_c. Influencing parameters were combined and adjusted repeatedly by trial and error until a relatively high correlation coefficient (R^2 = 0·97) was achieved. As a result, the following equation for v_c was obtained (Figure 2)

$$v_c = 0{\cdot}79 \exp\left[-0{\cdot}03\left(\frac{f_c'}{f_{co}}\right)^{0{\cdot}9}\left(\frac{\rho_o}{\rho_c}\right)^{1{\cdot}6}\right] \quad (7)$$

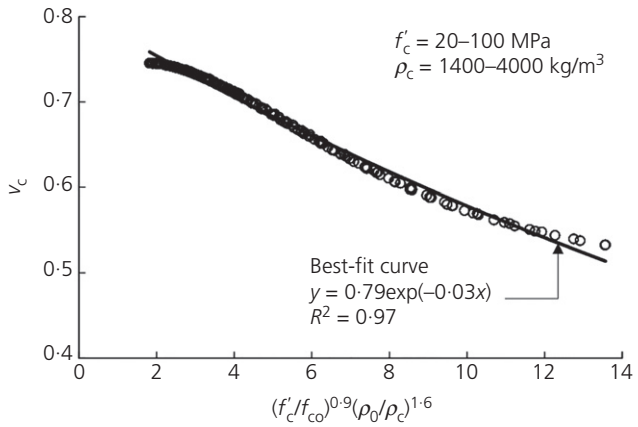

Figure 2. Modelling of v_c for different concretes

where f_{co} (= 10 MPa) and ρ_o (= 2300 kg/m^3) are respectively the reference values for the compressive strength and unit weight of concrete.

The effective strength ratio (f_t^*/f_c^*) required for the estimation of parameters l and m in Equations 3 and 4 was solved using the compressive stress–strain relationship of Yang *et al.* (2014) and the tensile stress–strain relationship proposed by Hordijk (1991). From NLMR analysis of the mathematical results obtained from Equations 5 and 6 for concrete with f_c' = 20–100 MPa, ρ_c = 1400–4000 kg/m^3 and aggregate size (d_a) between 5 and 25 mm, f_t^*/f_c^*, plotted in Figure 3, can be simply expressed as

$$8. \quad \frac{f_t^*}{f_c^*} = 0{\cdot}064\left[\left(\frac{f_c'}{f_{c0}}\right)\left(\frac{c_0}{d_a}\right)^{1{\cdot}7}\left(\frac{\rho_c}{\rho_o}\right)^{0{\cdot}1}\right]^{-0{\cdot}43}$$

where c_0 (= 25 mm) is the reference value for the maximum aggregate size.

Angle of concrete friction

Kahraman and Altindag (2004) pointed out that the concrete friction angle (ϕ) commonly increases with an increase in material brittleness. In the case of sliding failure of a modified Coulomb material under pure shear stress, the shear stress along the failure plane of the concrete interface can be expressed as (Yang *et al.*, 2012)

$$9. \quad \tau_n = \frac{f_c^* \cos\phi}{2\sqrt{k}}$$

where the quantity k is defined by $(1 + \sin\phi)/(1 - \sin\phi)$. For a concrete interface without transverse reinforcement and additional axial loads, the shear friction strength can be written, using Equation 3, in the following form

$$10. \quad \tau_n = \frac{1}{2} f_c^* \frac{1}{\cos\alpha}(l - m\sin\alpha)$$

At failure of concrete interfaces, the shear stresses obtained from Equation 9 should be the same as that calculated from Equation 10, and consequently ϕ can be obtained from

$$11. \quad \phi = \cos^{-1}\left(\frac{l - m\sin\alpha}{\cos\alpha}\sqrt{\frac{1+\sin\phi}{1-\sin\phi}}\right)$$

Equation 11 indicates that ϕ varies depending on the value of f_t^*/f_c^*. For common values of f_t^*/f_c^* within the range 0·01–0·06, the variation of ϕ determined from numerical analysis of Equation 11 is plotted in Figure 4. Hence, ϕ can be proposed as a function of f_t^*/f_c^* using simple linear regression analysis as

$$12. \quad \phi = 20{\cdot}65\left(\frac{f_t^*}{f_c^*}\right)^{-0{\cdot}21}$$

Database of monolithic concrete interfaces

A total of 103 test specimens providing the shear friction strength of monolithic concrete interfaces were compiled from different experimental sources (Ahmed and Ansell, 2010; Hofbeck *et al.*, 1969; Hwang and Yang, 2016; Mattock, 1976; Mattock and Hawkins, 1972; Mattock *et al.*, 1976; Yang *et al.*, 2012). All the specimens were tested under push-off loading conditions to simulate the shear friction behaviour at the monolithic interfaces of two elements. As a result, all of the push-off specimens were reported to have failed in shear friction along the interface. For all the push-off specimens, the Appendix lists

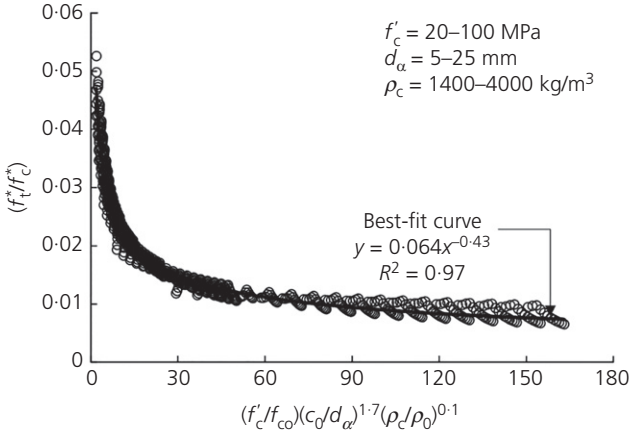

Figure 3. Modelling of f_t^*/f_c^* for different concretes

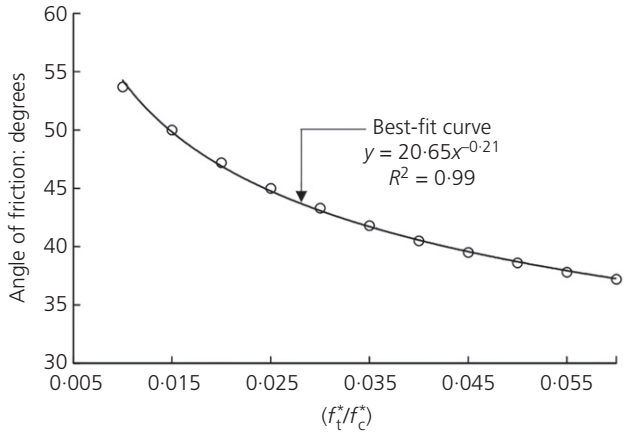

Figure 4. Variation of ϕ against f_t^*/f_c^*

Parameter and range	Incidence in database		
	Lightweight concrete (LWC)	Normal-weight concrete (NWC)	Heavyweight concrete (HWC)
A_c: mm^2			
20 000 to 25 000	8	4	—
25 000 to 30 000	—	—	—
30 000 to 35 000	21	56	3
35 000 to 40 000	—	—	—
40 000 to 50 000	—	5	—
50 000 to 60 000	—	6	—
f'_c: MPa			
10 to 20	—	4	—
20 to 30	21	46	—
30 to 40	8	5	—
40 to 50	—	10	—
50 to 60	—	—	3
60 to 70	—	6	—
ρ_{vf}			
0	11	9	1
0·001 to 0·01	6	23	2
0·01 to 0·02	6	25	—
0·02 to 0·03	6	11	—
0·03 to 0·04	—	3	—
ω_v (=(ρ_{vf} f_y)/f'_c)			
0	11	9	1
0·01 to 0·05	—	2	—
0·05 to 0·10	3	13	2
0·10 to 0·15	3	12	—
0·15 to 0·25	6	18	—
0·25 to 0·35	6	17	—
σ_x: MPa			
15 to 10	—	3	—
10 to 5	—	3	—
5 to 0	—	4	—
0	29	57	3
0 to −5	—	4	—
σ_x/f'_c			
0·3 to 0·2	—	3	—
0·2 to 0·1	—	7	—
0·1 to 0	—	—	—
0	29	57	3
0 to − 0·1	—	4	—

Table 1. Incidence of various parameter values in the compiled database

the area of the failure plane, maximum aggregate size, concrete strength and type, axial stresses and reinforcement details at the interfacial shear plane. Table 1 lists the distribution of various parameter values in the compiled database. The concrete type according to ρ_c was classified into three groups: LWC (29 specimens) for ρ_c between 1400 and 2100 kg/m^3, NWC (71 specimens) for ρ_c between 2101 and 2500 kg/m^3 and HWC (3 specimens) for ρ_c exceeding 2500 kg/m^3. Table 1 shows that the number of HWC test specimens was very limited. Most of the LWC specimens were produced using artificially expanded clay granules of dry density less than 1·65 g/cm^3. HWC specimens with $f'_c = 58{\cdot}8$ MPa were

Model	Shear friction capacity of concrete interfaces
ACI (2014)	$\tau_n = V_n/A_v = \rho_{vf} f_y (\mu\lambda \sin\theta_s + \cos\theta_s)$; $\mu = 1{\cdot}4$ for monolithic cast $\tau_n \le \min[0{\cdot}2f'_c, (3{\cdot}3 + 0{\cdot}08f'_c)]$ for NWC with $\lambda = 1{\cdot}0$ $\tau_n \le \min(0{\cdot}2f_{ck}, 5{\cdot}5)$ for sand LWC with $\lambda = 0{\cdot}85$ and all LWC with $\lambda = 0{\cdot}75$
Aashto (2012)	$\tau_n = c + \mu(\rho_{vf} f_y + \sigma_x) \le \min(0{\cdot}25f'_c, T_2)$ $c = 2{\cdot}76$ MPa, $\mu = 1{\cdot}4$ and $T_2 = 10{\cdot}34$ MPa for NWC $c = 1{\cdot}65$ MPa, $\mu = 1{\cdot}0$ and $T_2 = 6{\cdot}89$ MPa for LWC
Shaikh (1978)	$\tau_n = 3{\cdot}12\lambda\sqrt{\rho_{vf} f_y}$ $\lambda = 1{\cdot}0$ for NWC, 0·85 for sand LWC and 0·75 for all LWC
Walraven *et al*. (1987)	$\tau_n = C_1(\rho_{vf} f_y)^{C_2}$ $C_1 = 0{\cdot}822(f'_c/0{\cdot}85)^{0{\cdot}406}$ and $C_2 = 0{\cdot}159(f'_c/0{\cdot}85)^{0{\cdot}303}$
Loov and Patnaik (1994)	$\tau_n = 0{\cdot}6\lambda\sqrt{(0{\cdot}1 + \rho_{vf} f_y) f_{ck}} \le 0{\cdot}25 f_{ck}$ $\lambda = 1{\cdot}0$ for NWC, 0·85 for sand LWC and 0·75 for all LWC
Mattock (2001)	$\tau_n = K_1 + 0{\cdot}8(\rho_{vf} f_y + \sigma_x) \le \min(K_2 f'_c, K_3)$ for $\rho_{vf} f_y + \sigma_x \ge K_1/1{\cdot}45$ $\tau_n = 2{\cdot}25(\rho_{vf} f_y + \sigma_x)$ for $\rho_{vf} f_y + \sigma_x \le K_1/1{\cdot}45$ $K_1 = 0{\cdot}1 f'_c \le 5{\cdot}5$ MPa, $K_2 = 0{\cdot}3$ and $K_3 = 16{\cdot}5$ MPa for NWC $K_1 = 1{\cdot}7$ for sand LWC and 1·4 for all LWC $K_2 = 0{\cdot}2$ and $K_3 = 8{\cdot}3$ MPa for LWC
This study	$\tau_n = \frac{1}{2} f^*_c \frac{1}{\cos\alpha}(l - m\sin\alpha) + \rho_{vf} f_y \frac{\cos(\theta_s - \alpha)}{\cos\alpha} + \sigma_x \tan\alpha$ $l = 1 - 2\frac{f^*_t}{f^*_c}\frac{\sin\phi}{1-\sin\phi}$, $m = 1 - 2\frac{f^*_t}{f^*_c}\frac{1}{1-\sin\phi}$, $\phi = 20{\cdot}65\left(\frac{f^*_t}{f^*_c}\right)^{-0{\cdot}21}$ $\frac{f^*_t}{f^*_c} = 0{\cdot}064\left[\left(\frac{f'_c}{f_{co}}\right)\left(\frac{c_0}{d_a}\right)^{1{\cdot}7}\left(\frac{\rho_c}{\rho_o}\right)^{0{\cdot}1}\right]^{-0{\cdot}43}$ $\alpha = \sin^{-1}\left[\frac{1}{l}\left(m - \frac{2(\rho_{vf} f_y \sin\theta_s + \sigma_x)}{f^*_c}\right)\right]$ $v_c = 0{\cdot}79\exp\left[-0{\cdot}03\left(\frac{f'_c}{f_{co}}\right)^{0{\cdot}9}\left(\frac{\rho_o}{\rho_c}\right)^{1{\cdot}6}\right]$

Table 2. Summary of previous equations and proposed mechanism model

produced using magnetite aggregate particles of density greater than 3·79 g/cm^3. The range of f'_c was 25·8–36·2 MPa for LWC and 16·4–62·5 MPa for NWC. No transverse reinforcement at the interfacial shear plane was provided in 17 specimens. For the reinforced specimens, ρ_{vf} varied between 0·001 and 0·040, producing a transverse reinforcement capacity ($\rho_{vf} f_y$) of 1·45–10·38 MPa. Most specimens were not subjected to additional axial stresses; ten specimens were subjected to additional compressive stresses and four specimens were subjected to additional tensile stresses.

Comparison of prediction models and test results

Review of existing equations

Most available equations to evaluate the shear friction capacity of concrete interfaces are based on friction action (Aashto, 2012; ACI, 2014; Shaikh, 1978) along the interfacial shear plane or on empirical equations (Loov and Patnaik, 1994; Mattock, 2001; Walraven *et al*., 1987) determined from regression analysis of limited test data, as summarised in Table 2. The ACI 318-14 equation (ACI, 2014) ignores concrete cohesion and assumes that the applied shear force is entirely transferred by the friction action of transverse reinforcement, which is assumed to be equal to $\mu\rho_{vf} f_y$, where μ is the coefficient of friction. Hence the frictional resistance provided by the transverse reinforcement depends on the roughness of the interfacial shear plane. For LWC interfacial shear planes, ACI 318-14 introduces a modification factor (λ) to compensate for the reduced aggregate interlock due to the rupture of lightweight aggregate particles. ACI 318-14 also imposes a limiting value on τ_n as a function of concrete shear resistance to avoid overestimation of concrete interfaces with over-reinforcement or high-strength concrete. This implies that stresses in

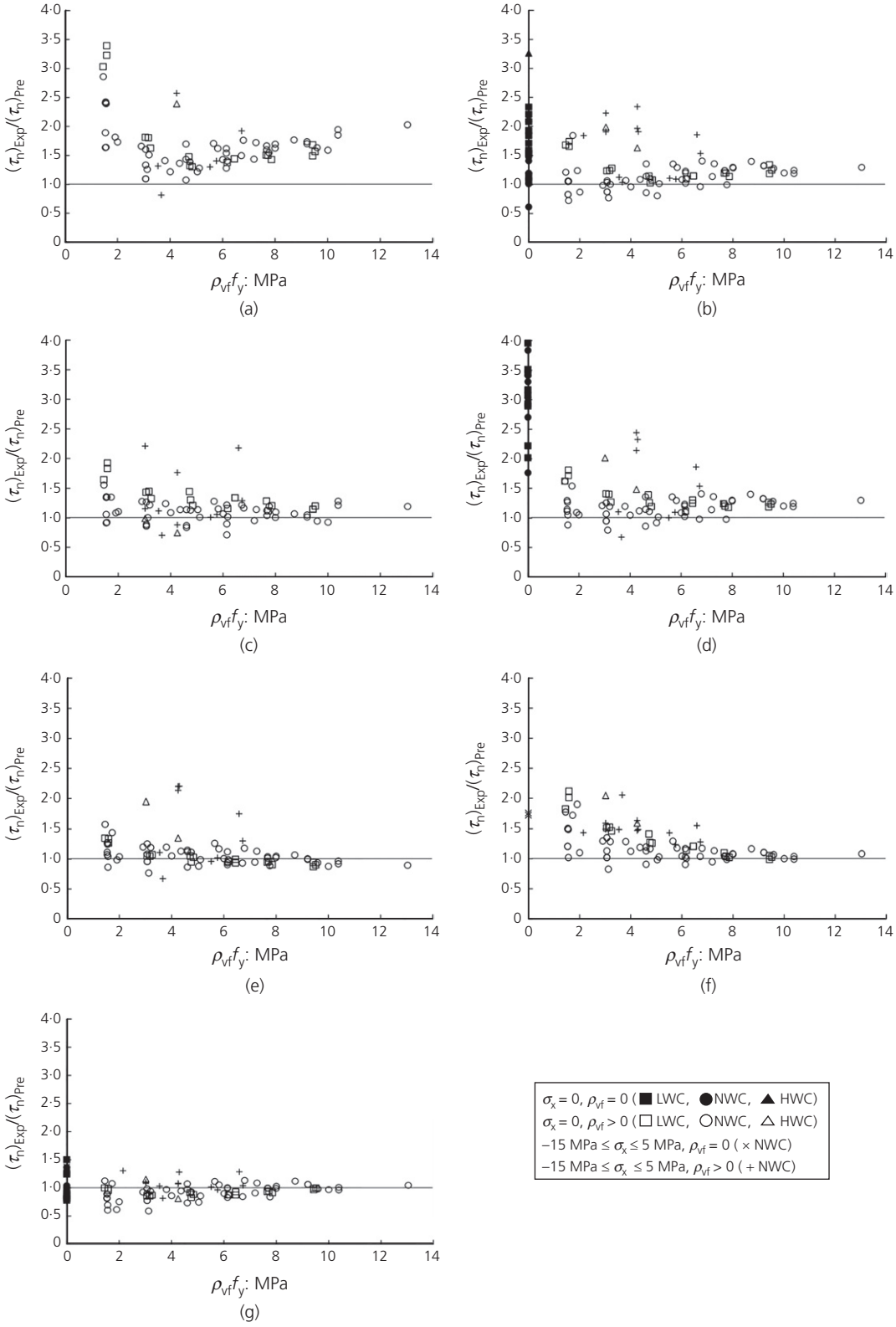

Figure 5. Comparison of measured and predicted shear friction capacities: (a) ACI (2014); (b) Aashto (2012); (c) Shaikh (1978); (d) Loov and Patnaik (1994); (e) Walraven *et al*. (1987); (f) Mattock (2001); (g) this study

transverse reinforcement should reach yield strength before crushing of concrete at the interface. Aashto (2012) considers τ_n as a summation of concrete cohesion and frictional resistance of the transverse reinforcement. All transverse reinforcing bars are assumed to be perpendicularly arranged to the interface. For monolithic interfaces, the concrete cohesion and coefficient of friction are set at 2·76 MPa and 1·4, respectively, for NWC and 1·65 MPa and 1·0, respectively, for LWC. The concrete cohesion is regarded to be independent of f'_c.

Shaikh (1978) proposed τ_n as a root function of the shear transfer capacity of transverse reinforcement on the basis of regression analysis of limited test data. Walraven *et al.* (1987) determined experimental parameters for shear friction using push-off test data; the experimental parameters for NWC were generalised as a function of f'_c. Loov and Patnaik (1994) set the μ value at 0·6 for a monolithic interface and considered the effect of f'_c on τ_n. Loov and Patnaik (1994) limited τ_n not to exceed $0{\cdot}25f'_c$ through comparisons with limited test results and the proposed equation. Hence, τ_n predicted by the Loov and Patnaik (1994) equation is governed by the concrete transfer capacity when the transverse reinforcement index (ω_v) is greater than 0·07 for NWCs and 0·16 for all LWCs. This implies that the concrete crushing resistance at the interface is higher for LWC than for NWC. However, the crack propagation resistance and tensile capacity of LWC are commonly lower than those of NWC having the same compressive strength (Choi *et al.*, 2014). Mattock (2001) reviewed the effect of various parameters (including f'_c, ρ_{vf} and σ_x) on τ_n using push-off specimens compiled from different sources to propose alternatives to the ACI equation. For the empirically developed equations for τ_n, Mattock (2001) determined the experimental constants from regression analysis using test data with f'_c ranging from 17 MPa to 100 MPa. In the database, only nine specimens were subjected to additional axial stresses. The Mattock equation also ignores the shear transfer contribution of concrete when $\rho_{vf} f_y + \sigma_x$ is less than $K_1/1{\cdot}45$, where K_1 is a constant related to concrete cohesion (see Table 2). Thus, for NWC interfaces with f'_c less than 55 MPa and without σ_x, τ_n proportionally increases with $\rho_{vf} f_y$ when the transverse reinforcement index ($\omega_v = \rho_{vf} f_y/f'_c$) does not exceed 0·069.

All of the previously developed equations presented in Table 2 commonly consider the shear transfer of transverse reinforcement as a primary mechanism of shear frictional resistance at interfacial shear planes. For over-reinforced interfaces, the upper limit is applied in terms of the maximum crushing resistance of concrete. This implies that τ_n remains constant when $\rho_{vf} f_y$ exceeds a certain limit. Walraven *et al.* (1987) did not account for the reduced shear transfer capacity of LWC. The equations proposed by Aashto (2012) and Mattock (2001) assume that the contribution of σ_x to τ_n is equal to that of $\rho_{vf} f_y$, although this equivalent contribution is invalid for an interface subjected to additional tensile stresses.

Comparisons with test results

Figure 5 shows comparisons of the measured shear friction capacities of the push-off specimens in the database and those predicted by the proposed mechanism model and the previous equations summarised in Table 2. The mean (γ_m), standard deviation (γ_s) and coefficient of variation (γ_v) of the ratios of experimental and predicted shear friction capacities ($\gamma = (\tau_n)_{Exp}/(\tau_n)_{Pre}$) are also compared in Table 3 for different groups divided according to concrete unit weight and the existence of transverse reinforcement and additional axial stresses. The value of μ for HWC in the previous equations was assumed to be the same as the value specified for NWC. The specimens without transverse reinforcement were excluded from the comparisons using the equations of ACI 318-14 (ACI, 2014), Shaikh (1978) and Walraven *et al.* (1987), as these equations neglect the shear transfer capacity of concrete cohesion. It is to be noted that values of the ratio γ below 1·0 indicate an unsafe prediction of the shear friction strength, whereas values of γ exceeding 1·0 show a safe prediction. Important findings emerging from the comparisons are now discussed.

The ACI 318-14 equation (ACI, 2014) considerably underestimates the shear friction capacity of the concrete interface with transverse reinforcement (Figure 5(a)), because concrete cohesion is not considered and the shear transfer capacity of the transverse reinforcement is limited by an upper bound when ω_v is more than 0·14 for normal-strength NWC and 0·19 for normal-strength LWC. The Aashto equation (Aashto, 2012) also gives an underestimation of results (Figure 5(b)), regardless of the type of concrete, yet the conservatism is lower than that determined from ACI 318-14 (ACI, 2014). This underestimation tends to increase with increases in concrete unit weight and compressive axial stresses. The lack of safety of the Aashto equation can also be observed for NWC specimens with $\rho_{vf} f_y$ less than 8 MPa. The equations proposed by Shaikh (1978) (Figure 5(c)) and Loov and Patnaik (1994) (Figure 5(d)) produced similar results for specimens with transverse reinforcement. The equation of Loov and Patnaik (1994) considerably underestimates the shear transfer capacity of concrete, which results in very high values of γ_m for specimens without transverse reinforcement. The equation of Walraven *et al.* (1987) (Figure 5(e)) gives lower values of γ_s and γ_v than the other equations, revealing a narrow scatter, although reduced aggregate interlock is not considered for LWC. However, the values of γ_m and γ_s determined from the Walraven *et al.* (1987) equation sharply increase for NWC specimens subjected to additional axial stresses. The equation proposed by Mattock (2001) (Figure 5(f)) for specimens with transverse reinforcement has values of γ_m and γ_s close to the equations of Shaikh (1978) and Loov and Patnaik (1994), but the Mattock equation has more accuracy for specimens with additional axial stresses. This is because the regression analysis conducted by Mattock involved push-off specimens subjected to constant axial stresses. The γ value of Mattock's equation tends to slightly decrease with an increase in $\rho_{vf} f_y$.

Group according to σ_x (MPa) and ρ_{vf}	Statistical value	Model						
		ACI (2014)	Aashto (2012)	Shaikh (1978)	Walraven *et al.* (1987)	Loov and Patnaik (1994)	Mattock (2001)	This study
Lightweight concrete (LWC)								
$\sigma_x = 0$	γ_m	—	1·73	—	—	3·38	—	0·98
$\rho_{vf} = 0$	γ_s	—	0·40	—	—	0·98	—	0·24
$\sigma_x = 0$	γ_m	1·80	1·27	1·36	1·03	1·34	1·34	0·92
$\rho_{vf} > 0$	γ_s	0·67	0·21	0·23	0·14	0·19	0·34	0·06
Subtotal	γ_m	1·80	1·44	1·36	1·03	2·12	1·34	0·95
	γ_s	0·67	0·37	0·23	0·14	1·18	0·34	0·15
	γ_v	0·37	0·26	0·17	0·14	0·56	0·25	0·16
Normal-weight concrete (NWC)								
$\sigma_x = 0$	γ_m	—	1·27	—	—	3·17	—	1·00
$\rho_{vf} = 0$	γ_s	—	0·46	—	—	0·78	—	0·17
$-3 \le \sigma_x \le 12$	γ_m	—	1·51	—	—	10·94	1·51	1·17
$\rho_{vf} = 0$	γ_s	—	0·35	—	—	0·29	0·35	0·29
$\sigma_x = 0$	γ_m	1·68	1·13	1·13	1·06	1·18	1·15	0·92
$\rho_{vf} > 0$	γ_s	0·52	0·21	0·26	0·15	0·17	0·20	0·13
$-3 \le \sigma_x \le 12$	γ_m	3·25	1·64	1·99	1·76	1·85	1·50	1·14
$\rho_{vf} > 0$	γ_s	2·28	0·43	1·33	0·75	0·77	0·22	0·20
Subtotal	γ_m	2·03	1·25	1·33	1·21	1·61	1·25	0·97
	γ_s	1·27	0·34	0·72	0·45	1·72	0·27	0·17
	γ_v	0·62	0·27	0·54	0·37	1·07	0·22	0·18
Heavyweight concrete (HWC)								
$\sigma_x = 0$	γ_m	3·52	1·81	0·87	1·65	1·75	1·82	0·98
$\rho_{vf} > 0$	γ_s	1·60	0·25	0·17	0·43	0·38	0·32	0·24
Total								
	γ_m	1·98	1·33	1·34	1·17	1·90	1·27	0·97
	γ_s	1·16	0·41	0·64	0·41	1·63	0·29	0·17
	γ_v	0·59	0·31	0·48	0·35	0·86	0·23	0·17

Table 3. Comparison of statistical values obtained from γ ($=(\tau_n)_{Exp}/(\tau_n)_{Pre}$) values of each model

In summary, the preceding comparisons reveal the following limitations of the previous empirical equations.

- The shear transfer capacity by concrete cohesion along the interface is considerably underestimated.
- The underestimation increases for an interface subjected to additional axial stresses.
- The accuracy is sensitive to concrete unit weight, resulting in large deviations for LWC.
- The inclination of transverse reinforcement to the interface is not considered in the equations formulated from the regression analysis using test data.

The predictions from the model proposed in this study are in better agreement with the test results, regardless of the concrete unit weight and amount of transverse reinforcement (Figure 5(g)). The overall values of $\gamma_m = 0{\cdot}97$ and $\gamma_s = 0{\cdot}17$ were the lowest values obtained. Moreover, the proposed model produced the best accuracy for specimens with additional axial stresses. The cohesion and coefficient of friction for concrete with different unit weights and compressive strengths can be evaluated using the equations derived from the proposed mechanism analysis. Ultimately, the proposed model provides superior accuracy in predicting the shear frictional capacity of interfaces constructed using various concretes.

Verification of primary influencing parameters

The influence of primary parameters on the shear friction strength (τ_n) of the interfaces was studied using the proposed model and the Aashto equation (Aashto, 2012) as well as appropriate experimental results from the database. To examine whether the code provisions reasonably consider the influencing parameters, the Aashto equation, having lower γ_s values than the ACI 318-14 equation (ACI, 2014), was selected. In a

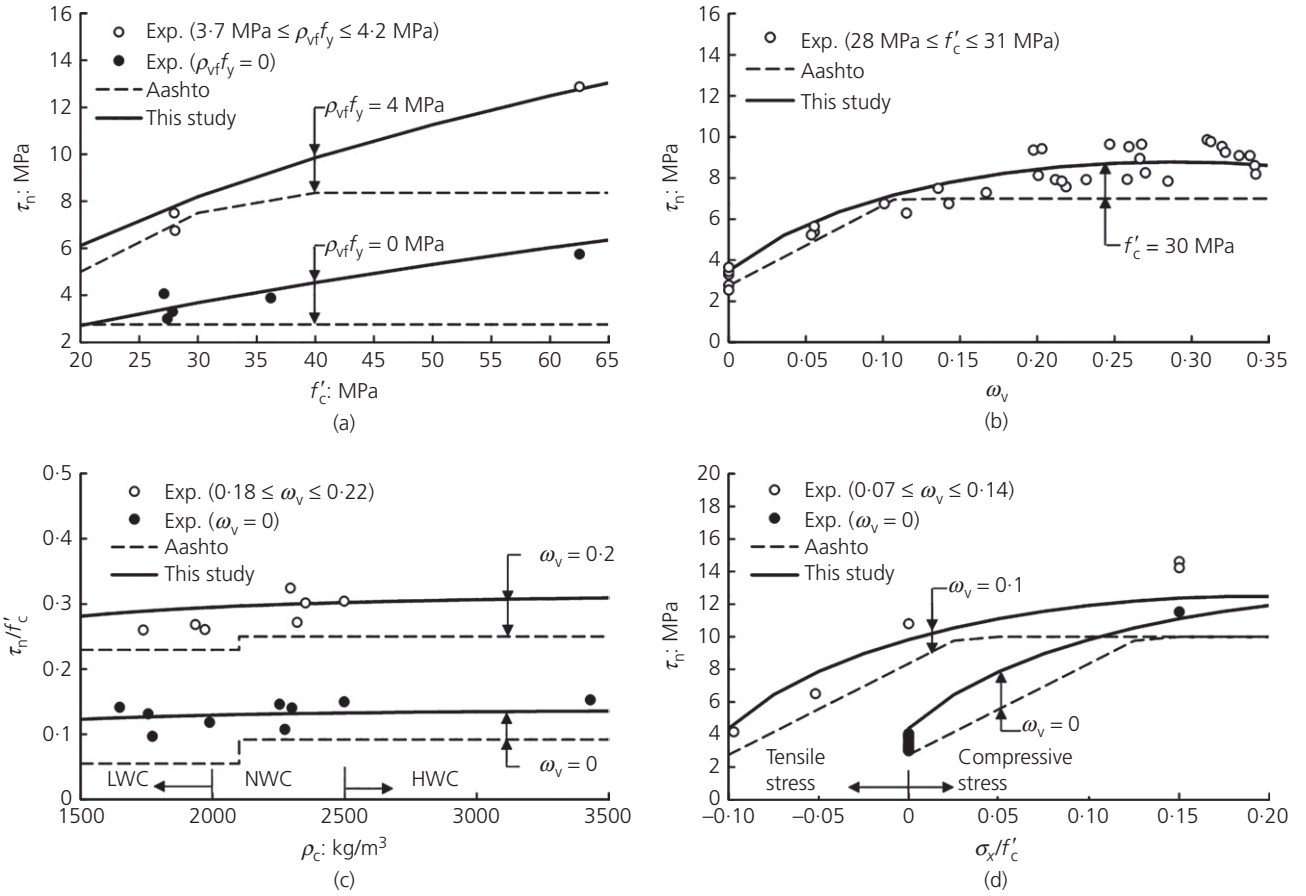

Figure 6. Effect of different parameters on shear friction strength: (a) compressive strength of NWC; (b) Transverse reinforcement ratio; (c) unit weight of concrete; (d) additional axial stress

parametric study, one parameter is incrementally changed, while the others are kept constant. However, as the test results in the database were collected from different sources, it was not possible to strictly achieve this and average values of concrete and steel reinforcement properties were thus used.

Figure 6(a) shows the effect of f'_c on the shear friction strength of NWC interfaces without additional axial stresses. For interfaces without transverse reinforcement, the Aashto equation gives a constant value of 2·76 MPa for NWC and 1·65 MPa for LWC, regardless of the variation of f'_c, indicating that concrete cohesion is independent of f'_c. For interfaces with transverse reinforcement, τ_n of the Aashto equation increases up to a certain limit, beyond which it remains constant. The value of τ_n depends on f'_c when τ_n is governed by the upper limit of $0{\cdot}25f'_c$. The kink point of τ_n against f'_c varies according to the value of ρ_{vf} f_y. The Aashto equation underestimates the shear transfer capacity by concrete cohesion. Meanwhile, τ_n predicted by the model proposed in this study increases with an increase in f'_c, showing a greater slope of increasing rate for interfaces with transverse reinforcement, as also demonstrated by test results.

The effect of ω_v on τ_n of NWC interfaces without additional axial stresses is shown in Figure 6(b). The value of τ_n determined from the Aashto equation increases with an increase of ω_v up to a certain limit, beyond which τ_n remains constant as the shear transfer capacity of over-reinforced interfaces is regarded to be governed by concrete crushing. The underestimation of the Aashto equation becomes notable when ω_v is greater than about 0·1 because of the upper limit. On the other hand, the predictions obtained from the proposed model increase with an increase in ω_v, indicating that the increasing rate is gradually alleviated. For over-reinforced interfaces, the proposed model shows a better accuracy compared with experimental results.

The effect of ρ_c on τ_n of interfaces without additional axial stresses is shown in Figure 6(c). The Aashto equation does not differentiate between NWC and HWC and applies the

Researcher and specimen ID	Concrete type	A_c: mm^2	d_a: mm	f'_c: MPa	$\rho_{vf}\,f_y$: MPa	σ_x: MPa	$(\tau_n)_{Exp}$	$(\tau_n)_{Pre}$							$(\tau_n)_{Exp}/(\tau_n)_{Pre}$						
							(1)	(2)	(3)	(4)	(5)	(6)	(7)	(8)	(1)/(2)	(1)/(3)	(1)/(4)	(1)/(5)	(1)/(6)	(1)/(7)	(1)/(8)
Hofbeck *et al*. (1969)																					
1·0	NWC	32 258	22	27·8	0·0000	0	3·31	0·00	2·76	0·00	0·00	1·00	0·00	3·59	—	1·20	—	—	3·30	—	0·92
1·1A	NWC	32 258	22	27·0	1·5344	0	5·17	2·15	4·90	3·85	4·06	3·99	3·45	5·80	2·41	1·05	1·34	1·27	1·30	1·50	0·89
1·1B	NWC	32 258	22	23·0	1·4527	0	5·82	2·03	4·79	3·75	3·69	3·59	3·27	5·16	2·86	1·21	1·55	1·58	1·62	1·78	1·13
1·2A	NWC	32 258	22	26·5	3·0688	0	6·89	4·30	6·61	5·44	5·50	5·49	5·10	7·00	1·60	1·04	1·27	1·25	1·25	1·35	0·98
1·2B	NWC	32 258	22	28·8	2·9054	0	6·75	4·07	6·82	5·30	5·63	5·58	5·20	7·28	1·66	0·99	1·27	1·20	1·21	1·30	0·93
1·3A	NWC	32 258	22	26·5	4·6032	0	7·58	5·29	6·61	6·67	6·61	6·61	6·33	7·77	1·43	1·15	1·14	1·15	1·15	1·20	0·98
1·3B	NWC	32 258	22	27·0	4·3580	0	7·37	5·40	6·75	6·49	6·53	6·58	6·19	7·79	1·36	1·09	1·14	1·13	1·12	1·19	0·95
1·4A	NWC	32 258	22	31·1	6·1376	0	9·37	5·79	7·77	7·70	8·36	7·77	8·02	9·31	1·62	1·21	1·22	1·12	1·21	1·17	1·01
1·4B	NWC	32 258	22	26·6	5·8107	0	8·61	5·31	6·64	7·49	7·35	6·64	7·30	8·15	1·62	1·30	1·15	1·17	1·30	1·18	1·06
1·5A	NWC	32 258	22	31·1	7·6720	0	9·65	5·79	7·77	8·61	9·29	7·77	9·24	9·64	1·67	1·24	1·12	1·04	1·24	1·04	1·00
1·5B	NWC	32 258	22	28·0	7·2634	0	9·54	5·54	7·00	8·38	8·43	7·00	8·40	8·76	1·72	1·36	1·14	1·13	1·36	1·13	1·09
1·6A	NWC	32 258	22	29·7	9·2064	0	9·87	5·68	7·42	9·43	9·80	7·42	8·91	9·27	1·74	1·33	1·05	1·01	1·33	1·11	1·06
1·6B	NWC	32 258	22	27·9	8·7161	0	9·78	5·53	6·98	9·18	9·14	6·98	8·37	8·73	1·77	1·40	1·07	1·07	1·40	1·17	1·12
2·1	NWC	32 258	22	21·4	1·5344	0	4·07	2·15	4·90	3·85	3·65	3·55	3·36	4·99	1·89	0·83	1·06	1·11	1·15	1·21	0·82
2·2	NWC	32 258	22	21·4	3·0688	0	4·69	4·27	5·34	5·44	4·89	4·94	4·59	6·04	1·10	0·88	0·86	0·96	0·95	1·02	0·78
2·3	NWC	32 258	22	26·9	4·6032	0	5·79	5·37	6·72	6·67	6·67	6·72	6·37	7·86	1·08	0·86	0·87	0·87	0·86	0·91	0·74
2·4	NWC	32 258	22	26·9	6·1376	0	6·89	5·37	6·72	7·70	7·60	6·72	7·60	8·30	1·28	1·03	0·89	0·91	1·03	0·91	0·83
2·5	NWC	32 258	22	28·8	7·6720	0	8·96	5·60	7·20	8·61	8·81	7·20	8·64	9·01	1·60	1·24	1·04	1·02	1·24	1·04	0·99
2·6	NWC	32 258	22	28·8	9·2064	0	9·54	5·60	7·20	9·43	9·59	7·20	8·64	8·98	1·70	1·33	1·01	1·00	1·33	1·10	1·06
3·2	NWC	32 258	22	27·6	1·5603	0	3·58	2·18	4·94	3·88	4·14	4·06	3·51	5·91	1·64	0·73	0·92	0·87	0·88	1·02	0·61
3·3	NWC	32 258	22	21·4	3·0688	0	4·69	4·27	5·34	5·44	4·89	4·94	4·59	6·04	1·10	0·88	0·86	0·96	0·95	1·02	0·78
3·4	NWC	32 258	22	27·8	5·1058	0	7·08	5·53	6·96	7·02	7·15	6·96	6·87	8·25	1·28	1·02	1·01	0·99	1·02	1·03	0·86
3·5	NWC	32 258	22	27·8	7·1891	0	7·94	5·53	6·96	8·33	8·36	6·96	8·35	8·70	1·44	1·14	0·95	0·95	1·14	0·95	0·91
4·1	NWC	32 258	22	28·0	2·0005	0	4·85	2·80	5·56	4·40	4·67	4·60	4·40	6·41	1·73	0·87	1·10	1·04	1·05	1·10	0·76
4·2	NWC	32 258	22	28·0	4·0009	0	6·75	5·54	7·01	6·22	6·42	6·43	6·00	7·82	1·22	0·96	1·09	1·05	1·05	1·12	0·86
4·3	NWC	32 258	22	29·9	6·0014	0	8·13	5·69	7·48	7·61	8·07	7·48	7·79	9·01	1·43	1·09	1·07	1·01	1·09	1·04	0·90
4·4	NWC	32 258	22	29·9	8·0018	0	9·65	5·69	7·48	8·79	9·23	7·48	8·97	9·35	1·69	1·29	1·10	1·05	1·29	1·08	1·03
4·5	NWC	32 258	22	30·2	10·0023	0	9·09	5·72	7·56	9·83	10·33	7·56	9·07	9·37	1·59	1·20	0·93	0·88	1·20	1·00	0·97
5·1	NWC	32 258	22	16·9	1·5344	0	3·51	2·15	4·22	3·85	3·27	3·15	2·92	4·26	1·64	0·83	0·91	1·07	1·11	1·21	0·82
5·2	NWC	32 258	22	18·1	3·0688	0	4·82	3·61	4·51	5·44	4·46	4·51	4·26	5·33	1·34	1·07	0·89	1·08	1·07	1·13	0·90
5·3	NWC	32 258	22	16·4	4·6032	0	5·58	3·29	4·11	6·67	4·96	4·11	4·93	5·19	1·70	1·36	0·84	1·12	1·36	1·13	1·07
5·4	NWC	32 258	22	17·8	6·1376	0	5·48	3·56	4·44	7·70	5·83	4·44	5·33	5·50	1·54	1·23	0·71	0·94	1·23	1·03	1·00
Mattock (1976)																					
A1	NWC	32 258	19	41·5	1·5628	0	5·24	2·19	4·94	3·89	5·02	4·98	3·52	7·49	2·39	1·06	1·35	1·04	1·05	1·49	0·70
A2	NWC	32 258	19	41·5	3·1257	0	5·51	4·38	7·13	5·49	7·18	6·94	6·65	9·30	1·26	0·77	1·00	0·77	0·79	0·83	0·59
A3	NWC	32 258	19	40·1	5·0344	0	7·92	6·51	9·80	6·97	8·98	8·61	8·04	10·58	1·22	0·81	1·14	0·88	0·92	0·99	0·75
A4	NWC	32 258	19	40·5	6·7126	0	9·78	6·54	10·13	8·05	10·48	9·97	9·42	11·54	1·50	0·97	1·21	0·93	0·98	1·04	0·85

Table 4. Basic data of existing specimens and comparison of predicted and measured shear friction strengths
(continued on next page)

Researcher and specimen ID	Concrete type	A_c: mm^2	d_a: mm	f'_c: MPa	$\rho_{vf}\ f_y$: MPa	σ_x: MPa	$(\tau_n)_{Exp}$	$(\tau_n)_{Pre}$							$(\tau_n)_{Exp}/(\tau_n)_{Pre}$						
							(1)	(2)	(3)	(4)	(5)	(6)	(7)	(8)	(1)/(2)	(1)/(3)	(1)/(4)	(1)/(5)	(1)/(6)	(1)/(7)	(1)/(8)
A5	NWC	32 258	19	42·2	7·7582	0	10·34	6·68	10·34	8·66	11·62	10·55	10·43	12·30	1·55	1·00	1·19	0·89	0·98	0·99	0·84
A6	NWC	32 258	19	40·7	10·3846	0	12·13	6·55	10·16	10·02	13·14	10·16	12·20	12·56	1·85	1·19	1·21	0·92	1·19	0·99	0·97
A6A	NWC	32 258	19	41·1	10·3846	0	12·82	6·59	10·28	10·02	13·26	10·28	12·34	12·69	1·94	1·25	1·28	0·97	1·25	1·04	1·01
A7	NWC	32 258	19	41·1	13·0348	0	13·37	6·59	10·28	11·22	14·90	10·28	12·34	12·73	2·03	1·30	1·19	0·90	1·30	1·08	1·05
Mattock and Hawkins (1972)																					
9·2	NWC	32 258	25	37·9	6·7948	−10·2	17·64	6·33	9·47	8·10	10·06	9·47	11·37	13·72	2·79	1·86	2·18	1·75	1·86	1·55	1·29
9·3	NWC	32 258	25	27·1	6·8078	−2·8	10·44	5·43	6·79	8·11	8·02	6·79	8·14	10·04	1·92	1·54	1·29	1·30	1·54	1·28	1·04
9·4	NWC	32 258	25	27·1	6·9900	0	9·57	5·43	6·79	8·22	8·11	6·79	8·14	8·43	1·76	1·41	1·16	1·18	1·41	1·18	1·13
9·5	NWC	32 258	25	44·4	4·4257	−11·4	19·77	5·37	10·34	6·54	8·97	8·50	13·31	15·45	3·69	1·91	3·02	2·20	2·33	1·49	1·28
9·6	NWC	32 258	25	44·4	2·2129	−11·0	19·09	2·68	10·34	4·62	6·22	6·08	13·31	14·62	7·11	1·85	4·13	3·07	3·14	1·43	1·31
Mattock *et al*. (1976)																					
A0	Sand LWC	32 258	9·5	29·1	0·0000	0	3·45	0·00	1·65	0·00	0·00	0·87	0·00	2·77	—	2·08	—	—	3·96	—	1·24
A1	Sand LWC	32 258	9·5	25·8	1·4469	0	5·22	1·72	3·10	3·18	3·87	3·22	2·86	5·21	3·03	1·68	1·64	1·35	1·62	1·83	1·00
A2	Sand LWC	32 258	9·5	28·2	3·2521	0	6·30	3·87	4·91	4·76	5·86	4·96	4·30	7·23	1·63	1·28	1·32	1·08	1·27	1·46	0·87
A3	Sand LWC	32 258	9·5	26·9	4·8368	0	7·03	5·39	6·49	5·81	6·83	5·88	5·57	7·94	1·30	1·08	1·21	1·03	1·19	1·26	0·88
A4	Sand LWC	32 258	9·5	28·2	6·1734	0	7·58	5·50	6·89	6·56	7·87	6·79	6·64	8·68	1·38	1·10	1·15	0·96	1·12	1·14	0·87
A5	Sand LWC	32 258	9·5	27·3	7·7168	0	8·20	5·46	6·82	7·34	8·51	6·82	7·87	8·70	1·50	1·20	1·12	0·96	1·20	1·04	0·94
A6	Sand LWC	32 258	9·5	29·3	9·4255	0	9·26	5·50	6·89	8·11	9·81	7·32	8·78	9·33	1·68	1·34	1·14	0·94	1·26	1·05	0·99
E0	All LWC	32 258	9·5	27·3	0·0000	0	3·86	0·00	1·65	0·00	0·00	0·74	0·00	2·57	—	2·33	—	—	5·19	—	1·50
E1	All LWC	32 258	9·5	28·6	1·5847	0	5·37	1·66	3·24	2·93	4·24	3·12	2·67	5·63	3·23	1·66	1·83	1·27	1·72	2·01	0·95
E2	All LWC	32 258	9·5	27·8	3·1694	0	6·01	3·33	4·82	4·15	5·74	4·29	3·94	7·00	1·81	1·25	1·45	1·05	1·40	1·53	0·86
E3	All LWC	32 258	9·5	28·0	4·7541	0	6·61	4·99	6·41	5·08	6·94	5·25	5·20	7·98	1·33	1·03	1·30	0·95	1·26	1·27	0·83
E4	All LWC	32 258	9·5	27·83	6·4490	0	7·92	5·50	6·89	5·92	7·95	6·08	6·56	8·51	1·44	1·15	1·34	1·00	1·30	1·21	0·93
E5	All LWC	32 258	9·5	28·4	7·6548	0	8·27	5·50	6·89	6·45	8·71	6·67	7·52	8·85	1·50	1·20	1·28	0·95	1·24	1·10	0·93
E6	All LWC	32 258	9·5	27·9	9·5151	0	8·61	5·50	6·89	7·19	9·52	6·98	8·37	8·60	1·57	1·25	1·20	0·90	1·23	1·03	1·00
G0	All LWC	32 258	12·7	27·8	0·0000	0	3·65	0·00	1·65	0·00	0·00	0·75	0·00	2·90	—	2·21	—	—	4·87	—	1·26
G1	All LWC	32 258	12·7	28·6	1·5847	0	5·65	1·66	3·24	2·93	4·23	3·12	2·67	5·71	3·40	1·74	1·93	1·33	1·81	2·12	0·99
G2	All LWC	32 258	12·7	26·7	3·0592	0	5·83	3·21	4·71	4·08	5·53	4·14	3·85	6·80	1·81	1·24	1·43	1·05	1·41	1·52	0·86
G3	All LWC	32 258	12·7	28·2	4·7128	0	7·30	4·95	6·37	5·06	6·95	5·25	5·17	7·99	1·48	1·15	1·44	1·05	1·39	1·41	0·91
G4	All LWC	32 258	12·7	30·5	6·4490	0	7·92	5·50	6·89	5·92	8·44	6·36	6·56	9·05	1·44	1·15	1·34	0·94	1·25	1·21	0·88
G5	All LWC	32 258	12·7	27·6	7·8546	0	7·85	5·50	6·89	6·53	8·65	6·67	7·68	8·58	1·43	1·14	1·20	0·91	1·18	1·02	0·92
G6	All LWC	32 258	12·7	27·6	9·4255	0	8·20	5·50	6·89	7·16	9·40	6·90	8·28	8·48	1·49	1·19	1·15	0·87	1·19	0·99	0·97
M0	NWC	32 258	12·7	27·1	0·0000	0	4·07	0·00	2·76	0·00	0·00	0·99	0·00	2·97	—	1·48	—	—	4·11	—	1·37
M1	NWC	32 258	12·7	28·8	1·5434	0	5·24	2·16	4·92	3·86	4·20	4·13	3·47	5·89	2·42	1·07	1·36	1·25	1·27	1·51	0·89
M2	NWC	32 258	12·7	26·9	3·1970	0	6·75	4·48	6·72	5·56	5·65	5·65	5·24	7·18	1·51	1·01	1·22	1·19	1·20	1·29	0·94
M3	NWC	32 258	12·7	27·5	4·7541	0	7·65	5·50	6·88	6·78	6·87	6·88	6·56	8·21	1·39	1·11	1·13	1·11	1·11	1·17	0·93
M4	NWC	32 258	12·7	28·6	6·1734	0	7·85	5·59	7·15	7·72	7·93	7·15	7·80	8·97	1·41	1·10	1·02	0·99	1·10	1·01	0·88
M5	NWC	32 258	12·7	27·1	7·9924	0	8·82	5·42	6·78	8·79	8·61	6·78	8·13	8·88	1·63	1·30	1·00	1·02	1·30	1·08	0·99
M6	NWC	32 258	12·7	28·4	9·5909	0	9·09	5·57	7·10	9·63	9·67	7·10	8·52	9·25	1·63	1·28	0·94	0·94	1·28	1·07	0·98

Table 4. Continued

Researcher and specimen ID	Concrete type	A_c: mm^2	d_a: mm	f'_c: MPa	$\rho_{vf}\ f_y$: MPa	σ_x: MPa	$(\tau_n)_{Exp}$	$(\tau_n)_{Pre}$						$(\tau_n)_{Exp}/(\tau_n)_{Pre}$						
							(1)	(2)	(3)	(4)	(5)	(6)	(7)	(8)	(1)/(2)	(1)/(3)	(1)/(4)	(1)/(5)	(1)/(6)	(1)/(7)	(1)/(8)
Mattock *et al*. (1975)																					
E1U	NWC	54 193	19	28·0	3·7974	0	7·50	5·32	6·99	6·06	6·26	6·26	5·84	7·70	1·41	1·07	1·24	1·20	1·20	1·29	0·97
E4U	NWC	54 193	19	26·6	3·5380	1·4	6·52	4·95	5·78	5·85	5·88	5·90	4·39	6·31	1·32	1·13	1·11	1·11	1·10	1·49	1·03
E6U	NWC	54 193	19	28·4	3·6605	2·8	4·18	5·12	4·02	5·95	6·21	6·20	2·04	5·12	0·82	1·04	0·70	0·67	0·67	2·05	0·82
F1U	NWC	54 193	19	27·8	5·6421	0	9·43	5·52	6·95	7·38	7·47	6·95	7·29	8·45	1·71	1·36	1·28	1·26	1·36	1·29	1·12
F4U	NWC	54 193	19	28·8	5·7502	1·4	7·88	5·60	7·19	7·45	7·71	7·19	6·37	8·16	1·41	1·10	1·06	1·02	1·10	1·24	0·97
F6U	NWC	54 193	19	29·2	5·5124	2·8	7·34	5·64	6·61	7·30	7·64	7·31	5·13	7·22	1·30	1·11	1·01	0·96	1·00	1·43	1·02
Yang *et al*. (2012)																					
A4	All LWC	24 000	4	31·2	0·0000	0	1·77	0·00	1·65	0·00	0·00	0·79	0·00	2·05	—	1·07	—	—	2·22	—	0·86
A8	All LWC	24 000	8	36·2	0·0000	0	2·63	0·00	1·65	0·00	0·00	0·86	0·00	2·88	—	1·59	—	—	3·08	—	0·91
A13	All LWC	24 000	13	31·8	0·0000	0	2·54	0·00	1·65	0·00	0·00	0·80	0·00	3·13	—	1·54	—	—	3·17	—	0·81
A19	All LWC	24 000	19	37·4	0·0000	0	3·06	0·00	1·65	0·00	0·00	0·87	0·00	3·92	—	1·85	—	—	3·51	—	0·78
S4	Sand LWC	24 000	4	34·8	0·0000	0	1·92	0·00	1·65	0·00	0·00	0·95	0·00	2·35	—	1·16	—	—	2·02	—	0·82
S8	Sand LWC	24 000	8	29·9	0·0000	0	2·55	0·00	1·65	0·00	0·00	0·88	0·00	2·63	—	1·54	—	—	2·89	—	0·97
S13	Sand LWC	24 000	13	36·0	0·0000	0	2·84	0·00	1·65	0·00	0·00	0·97	0·00	3·52	—	1·72	—	—	2·93	—	0·81
S19	Sand LWC	24 000	19	33·0	0·0000	0	3·19	0·00	1·65	0·00	0·00	0·93	0·00	3·73	—	1·93	—	—	3·45	—	0·85
N4	NWC	24 000	4	25·8	0·0000	0	1·70	0·00	2·76	0·00	0·00	0·96	0·00	1·90	—	0·62	—	—	1·76	—	0·89
N8	NWC	24 000	8	29·6	0·0000	0	2·79	0·00	2·76	0·00	0·00	1·03	0·00	2·68	—	1·01	—	—	2·70	—	1·04
N13	NWC	24 000	13	27·4	0·0000	0	3·01	0·00	2·76	0·00	0·00	0·99	0·00	2·98	—	1·09	—	—	3·03	—	1·01
N19	NWC	24 000	19	36·2	0·0000	0	3·89	0·00	2·76	0·00	0·00	1·14	0·00	4·15	—	1·41	—	—	3·41	—	0·94
Hwang and Yang (2016)																					
NH-N-0	NWC	31 500	25	62·5	0·0000	0	5·75	0·00	2·76	0·00	0·00	1·50	0·00	6·73	—	2·09	—	—	3·83	—	0·85
NH-V-0	NWC	31 500	25	62·5	4·2499	0	10·81	5·95	8·71	6·41	10·97	9·89	8·91	13·25	1·82	1·24	1·69	0·99	1·09	1·21	0·82
NH-X-0	NWC	31 500	25	62·5	3·0234	0	12·88	2·97	6·96	5·39	8·95	8·36	6·76	14·89	4·33	1·85	2·39	1·44	1·54	1·90	0·87
NH-N-0·15	NWC	31 500	25	62·5	0·0000	9·4	16·4	0·00	10·34	0·00	0·00	1·50	13·01	16·87	—	1·59	—	—	10·73	1·26	0·97
NH-V-0·15	NWC	31 500	25	62·5	4·2499	9·4	21·1	5·95	10·34	6·41	10·97	9·89	16·41	18·31	3·55	2·04	3·29	1·92	2·13	1·29	1·15
NH-X-0·15	NWC	31 500	25	62·5	3·0234	9·4	23·01	2·97	10·34	5·39	8·95	8·36	15·42	21·01	7·73	2·23	4·27	2·57	2·75	1·49	1·10
NN-N-0·15	NWC	31 500	25	29·8	0·0000	4·5	11·54	0·00	7·45	0·00	0·00	1·04	6·56	8·38	—	1·55	—	—	11·14	1·76	1·38
NN-V-0·15	NWC	31 500	25	29·8	4·2499	4·5	14·63	5·68	7·45	16·60	6·85	6·83	8·94	9·24	2·57	1·96	0·88	2·14	2·14	1·64	1·58
NN-X-0·15	NWC	31 500	25	29·8	3·0234	4·5	14·24	2·97	7·45	14·68	5·83	5·77	8·94	12·21	4·79	1·91	0·97	2·44	2·47	1·59	1·17
HH-N-0	HWC	31 500	25	58·8	0·0000	0	8·99	0·00	2·76	0·00	0·00	1·45	0·00	6·78	—	3·26	—	—	6·18	—	1·33
HH-V-0	HWC	31 500	25	58·8	4·2499	0	14·23	5·95	8·71	6·41	10·53	9·60	8·91	13·29	2·39	1·63	2·22	1·35	1·48	1·60	1·07
HH-X-0	HWC	31 500	25	58·8	3·0234	0	13·83	2·97	6·96	5·40	8·66	8·13	6·76	14·92	4·65	1·99	2·56	1·60	1·70	2·05	0·93

Table 4. Continued

same constants for concrete having $\rho_c > 2100$ kg/m^3. However, the aggregate interlock capacity and tensile resistance decrease with decreasing ρ_c (Choi *et al.*, 2014). This implies that the experimental constants for concrete shear capacity need to be formulated as a function of ρ_c or further subdivided according to ρ_c. The underestimation of the Aashto equation is more notable for LWC than for NWC. The test results showed that a slightly higher τ_n is observed for NWC interfaces than for LWC interfaces. The predictions obtained from the proposed model slightly increase as ρ_c increases, indicating that the slope of the increasing rate is independent of the amount of transverse reinforcement. There are no data available in the database for various concrete unit weights subjected to additional axial stresses. According to the proposed model, the increasing rate of τ_n with ρ_c is independent of the applied axial stresses.

The effect of σ_x on τ_n of NWC interfaces with $f'_c = 30$ MPa is shown in Figure 6(d). For the Aashto equation, a trend similar to the relationship between ω_v and τ_n is observed; namely, a further increase in τ_n is not expected for an interface without transverse reinforcement when σ_x/f'_c is greater than 0·125. The threshold point of σ_x/f'_c decreases with the increase in ω_v. The predictions obtained from the proposed model increase as σ_x increases, indicating a lower slope of the increasing rate for interfaces with transverse reinforcement.

Conclusions

An integrated model of monolithic concrete interfaces derived from the upper-bound theorem of concrete plasticity has been developed. The model is an extension to that presented in a previous investigation (Yang *et al.*, 2012) by considering the effects of applied axial stresses and transverse reinforcement. The angle of friction varying with concrete brittleness was expressed as a function of the effective strength ratio of f_t^*/f_c^*. The reliability and limitations of previous empirical equations and code provisions were examined through comparisons with test results of 103 push-off specimens compiled from different sources. The effect of various parameters on the shear friction strength of interfacial shear planes was also investigated using test results, the prediction models of Aashto (2012) and the model proposed in the present study. The following conclusions may be drawn.

(*a*) The previously proposed equations considerably underestimate the shear transfer capacity of concrete interfaces, especially those subjected to additional axial stresses. Furthermore, the accuracy of the previous equations exhibits high sensitivity to concrete unit weight, resulting in large deviations for lightweight concrete (LWC) interfaces.

(*b*) The proposed model provides superior accuracy in predicting the shear frictional capacity of interfaces constructed using various concretes, as indicated by the mean (0·97) and standard deviation (0·17) of the ratios of experimental and predicted shear friction strengths.

(*c*) The shear friction strength increases with an increase in concrete compressive strength. However, the increasing rate of shear friction strength is slightly larger for interfaces with transverse reinforcement.

(*d*) As the transverse reinforcement index increases, the shear friction strength increases. However, the increasing rate is gradually alleviated towards an upper limit of the shear friction strength.

(*e*) Compared with LWC interfaces, a slightly higher shear friction strength was observed for normal-weight concrete interfaces.

(*f*) According to the proposed model, the shear friction strength increases as axial compressive stresses increase, indicating a lower rate of increase for interfaces with transverse reinforcement.

Acknowledgement

This work was sponsored by Mid-Career Researcher Program (No. NRF-2014R1A2A2A09054557) and Basic Science Research Program (No. 2015R1A5A1037548) through the National Research Foundation of Korea (NRF) grant funded by the Ministry of Science, ICT & Future Planning (MSIP).

Appendix

Table 4 summarises test data of 103 push-off specimens and predicted shear friction strengths. The predictions obtained from the equations proposed by ACI (2014), Aashto (2012), Shaikh (1978), Walraven *et al.* (1987), Loov and Patnaik (1994) and Mattock (2001) are given in the columns labelled (2), (3), (4), (5), (6) and (7), respectively, and the prediction using the present model is given in the column labelled (8). The ratios between measured and predicted shear friction strengths using the reviewed models are also given in the table. The different parameters used in the table are defined in the notation.

REFERENCES

Aashto (American Association of State Highway and Transportation Officials) (2012) *Aashto LRFD Bridge Design Specifications*. Aashto, Washington, DC, USA.

ACI (American Concrete Institute) (2014) ACI 318-14: Building code requirements for structural concrete and commentary. ACI, Farmington Hills, MI, USA.

ACI-ASCE Committee 426 (1973) The shear strength of reinforced concrete members. *Journal of Structural Division ASCE* **99(6)**: 1091–1187.

Ahmed L and Ansell A (2010) Direct shear strength of high-strength fibre concrete. *Magazine of Concrete Research* **62(5)**: 379–390, http://dx.doi.org/10.1680/macr.2010.62.5.379.

Ali MA and White RN (1999) Enhanced contact model for shear friction of normal and high-strength concrete. *ACI Structural Journal* **96(3)**: 348–360.

Ashour AF and Morley CT (1994) The numerical determination of shear failure mechanisms in reinforced concrete beams. *The Structural Engineer* **72(23– 24)**: 395–400.

Choi SJ, Yang KH, Sim JI and Choi BJ (2014) Direct tensile strength of lightweight concrete with different specimen depths and aggregate sizes. *Construction and Building Materials* **63**: 132–141.

Exner H (1979) *On the Effectiveness Factor in Plastic Analysis of Concrete. Plasticity in Reinforced Concrete (Reports of the Working Commission)*. International Association of Bridge and Structural Engineering, Zurich, Switzerland.

Haskett M, Oehlers DJ, Mohamed Ali MS and Sharmat SK (2010) The shear friction aggregate interlock resistance across sliding planes in concrete. *Magazine of Concrete Research* **62(12)**: 907–924, http://dx.doi.org/10.1680/macr.2010.62.12.907.

Hofbeck JA, Ibrahim IO and Mattock AH (1969) Shear transfer in reinforced concrete. *ACI Structural Journal* **66(2)**: 119–128.

Hordijk DA (1991) *Local Approach to Fatigue of Concrete*. Doctoral dissertation, Delft University of Technology, Delft, the Netherlands.

Hwang YH and Yang KH (2016) Effect of transverse reinforcement and compressive stresses on the shear friction strength of concrete. *Journal of Korea Concrete Institute* **28(4)**: 419–426.

Kahraman S and Altindag R (2004) A brittleness index to estimate fracture toughness. *International Journal of Rock Mechanics and Mining Sciences* **41(2)**: 343–348.

Loov RE and Patnaik AK (1994) Horizontal shear strength of composite concrete beams with a rough interface. *PCI Journal* **39(1)**: 48–69.

Mattock AH (1976) *Shear Transfer Under Monotonic Loading: A Cross an Interface Between Concrete Cast at Different Times*. University of Washington, Seattle, WA, USA, Report SM76-3.

Mattock AH (2001) Shear friction and high-strength concrete. *ACI Structural Journal* **98(1)**: 50–59.

Mattock AH and Hawkins NM (1972) Shear transfer in reinforced concrete: recent research. *PCI Journal* **17(2)**: 76–93.

Mattock AH, Johal L and Chow HC (1975) Shear transfer in reinforced concrete moment or tension acting across the shear pane. *PCI Journal* **20(4)**: 76–93.

Mattock AH, Li WK and Wang TC (1976) Shear transfer in lightweight reinforced concrete. *PCI Journal* **32(1)**: 20–39.

Nielsen MP and Hoang LC (2011) *Limit Analysis and Concrete Plasticity*. CRC Press, Boca Raton, FL, USA.

Sagaseta J and Vollum RL (2011) Influence of aggregate fracture on shear transfer through cracks in reinforced concrete. *Magazine of Concrete Research* **63(2)**: 119–137, http://dx.doi.org/10.1680/macr.9.00191.

Shaikh AF (1978) Proposed revisions to shear-friction provisions. *PCI Journal* **23(2)**: 127–121.

Thorenfeldt E, Tomaszewicz A and Jensen JJ (1987) Mechanical properties of high strength concrete and application to design. *Proceedings of Symposium on the Utilization of High-Strength Concrete*. Tapir, Trondheim, Norway, pp. 149–159.

Walraven JC, Frenay J and Pruijssers A (1987) Influence of concrete strength and load history on the shear friction capacity of concrete members. *PCI Journal* **32(1)**: 66–84.

Yang KH, Sim JI, Kang JH and Ashour AF (2012) Shear capacity of monolithic concrete joints without transverse reinforcement. *Magazine of Concrete Research* **64(9)**: 767–779, http://dx.doi.org/10.1680/macr.11.00107.

Yang KH, Mun JH, Cho MS and Kang THK (2014) A stress–strain model for various unconfined concrete in compression. *ACI Structural Journal* **111(4)**: 819–826.

HOW CAN YOU CONTRIBUTE?

To discuss this paper, please submit up to 500 words to the editor at journals@ice.org.uk. Your contribution will be forwarded to the author(s) for a reply and, if considered appropriate by the editorial board, it will be published as a discussion in a future issue of the journal.